

# Refractive index changes in $n$ -type delta-doped GaAs under hydrostatic pressure

O. Oubram<sup>a</sup>, I. Rodríguez-Vargas<sup>b</sup>, and J. C. Martínez-Orozco<sup>b</sup>

<sup>a</sup>*Facultad de Ciencias Químicas e Ingeniería, Universidad Autónoma del Estado de Morelos,  
Av. Universidad 1001, Col. Chamilpa, 62209 Cuernavaca, Morelos, México.  
Phone: +52 01 777 329 7000 Ext. 7039; Fax: +52 01 777 329 7000 Ext. 7039  
e-mail: oubram@uaem.mx,*

<sup>b</sup>*Unidad Académica de Física, Universidad Autónoma de Zacatecas,  
Calzada Solidaridad Esquina con Paseo la Bufa S/N, Zacatecas, Zac., 98060, Mexico.*

Received 6 November 2013; accepted 17 February 2014

The effect of hydrostatic pressure on the refractive index changes (RIC) is studied in  $\delta$ -doped quantum well (DDQW) in GaAs. Based on the effective mass approximation we implement an algebraic formalism to calculate the electronic structure and RIC. Our results obtained with this model show that the position and the magnitude of the linear, nonlinear and total RIC are sensitive to hydrostatic pressure and bidimensional density. The incident optical intensity has a great effect on these optical quantities.

*Keywords:* Refractive index changes linear and nonlinear; hydrostatic pressure;  $\delta$ -doped quantum wells.

PACS: 78.20.Ci; 73.21.Fg; 74.62.F; 78.67.De; 61.50.Ks

## 1. Introduction

During the last decade there has been considerable interest on the linear and nonlinear optical properties of low-dimensional semiconductor structures, particularly those associated with intersubband transitions. Linear and nonlinear optical properties such as optical absorption [1–4] and refractive index changes (RIC) [2–5], have the potential for device applications in far-infrared detectors [6, 7], electro-optical modulators [8, 9], and infrared lasers [10].

Recent improvements in semiconductor growth techniques have made possible to prepare low-dimensional semiconductor structures with any desirable potential shape, such as quantum wells, quantum wires, and quantum dots [1, 4, 11–19]. It is to be noted that external factors such as shallow impurities, temperature, electric and magnetic fields, and pressure can change the linear and nonlinear optical and transport properties of nanostructures [3, 12, 13, 18, 20–26]. In the past few years, many researchers have studied the effect of the external factors on the electronic and optical properties of low dimensional semiconductor structures.

In particular, the linear and nonlinear optical properties of structures under hydrostatic pressure have been intensively studied both experimentally and theoretically by several authors:

From the experimental standpoint, Piechal *et al.* [25] have reported that laser diodes in (Al)InGaP can be tuned by pressure effects. Trzeciakowski *et al.* [27] have reported that pressure and temperature variations can change the band gap of III-V semiconductors, shifting the gain spectrum of laser diodes. Bajda and collaborators [29] studied the pressure and temperature dependence of gain in InGaAs/GaAs laser diodes, finding that pressure tuning is much more effective than temperature tuning. For further information about optical properties of nanostructures under hydrostatic pressure, the reader can refer to [25–29].

On the other hand, from the theoretical point of view, Liang and Xie [13] studied the combined effects of the hydrostatic pressure and temperature on optical properties of a hydrogenic impurity in the disc-shaped quantum dot, showing that pressure and temperature play an important role in the optical absorption coefficients and refractive index changes. Baghramyan *et al.* [30] studied the effects of hydrostatic pressure, temperature, electric field and aluminum concentration on the electronic states in GaAs/Ga<sub>1-x</sub>Al<sub>x</sub> As concentric double quantum rings. The effect of hydrostatic pressure on optical absorption and refractive index changes of a shallow hydrogenic impurity in a GaAs/GaAlAs quantum wire were discussed by Santhi and collaborators [31]. They reported a blue shift of the absorption resonant peak and of the total RIC due to pressure changes.

Recently, more attention has been paid to study the hydrostatic pressure applied to a two-dimensional structure. The results of optical properties in delta-doped system under hydrostatic pressure were analyzed by Martínez-Orozco *et al.* [20, 21], revealing that intermediate pressure leads to an enhancement of both nonlinear absorption and RIC, whereas for higher pressures the amplitudes of these quantities are significantly quenched. Eseauu [32] discussed the simultaneous effects of laser field and hydrostatic pressure on the intersubband transitions in square and parabolic quantum wells. The author found that the transitions between the ground and the first excited levels depends on the hydrostatic pressure. In fact, this dependence is responsible of the shifting in the linear and nonlinear optical properties [1, 4, 33, 34]. The simultaneous effects of hydrostatic pressure and magnetic field applied along the quantization direction on intersubband optical transitions in Pöschl-Teller quantum well are also investigated by Hakimyfarid *et al.* [35].

Within the mentioned context, the aim of our work is to study the effect of hydrostatic pressure on the linear and non-

linear refractive index changes (RIC) in GaAs DDQWs. It is worth mentioning that the theoretical methods, used to analyze this effect [23, 24, 36], can be cumbersome and time consuming. To this respect, we apply a simple theoretical model of hydrostatic pressure based on physical consideration to obtain readily the electronic structure and the linear and nonlinear RIC.

This paper is organized as follows: In the next section, details of the calculations of analytical expressions for the linear and nonlinear refractive index changes, using algebraic formalism, are presented. The results and discussion are presented in Sec. 3. Finally, in the last section, a brief conclusion is given.

## 2. Theoretical Background

In the effective mass approximation the Schrödinger equation for a  $n$ -type DDQW under hydrostatic pressure is given by:

$$\left( -\frac{\hbar^2}{2m^*(P)} \frac{d^2}{dz^2} + V(z, P) \right) \psi(z, P) = E(P) \psi(z, P), \quad (1)$$

where  $P$  is the hydrostatic pressure in units of kbar,  $V(z, P)$  is the pressure dependent confinement potential and  $m^*(P)$  is the pressure dependent effective mass. Usually, the electronic structure calculations in GaAs  $n$ -type DDQW can be carried out by solving a single band effective mass Schrödinger equation with a V-shaped Thomas-Fermi potential or by means of a self-consistent approach for each value of  $P$ .

A convenient way to perform such analysis is introducing effective atomic units. We suppose that at low hydrostatic pressure all physical properties can be expressed in terms of the effective Bohr radius and effective Rhydberg. In other way, the energies are given in units of the effective Rhydberg  $R_y^*(P)$  and distances are given in terms of the effective Bohr radius  $a_0^*(P)$ .

In term of dielectric constant  $\epsilon(P)$  and electron effective mass  $m^*(P)$  are given the effective Bohr radius  $a_0^*(P) = \epsilon(P)\hbar^2/m^*(P)e^2$  and the effective Rhydberg  $R_y^*(P) = e^2/2\epsilon(P)a_0^*(P)$ .

Furthermore, the energy, position, wave function and confinement potential can be written as:  $E(P) = E^* R_y^*(P)$ ,  $z = z^* a_0^*(P)$ ,  $\psi(z, P) = \psi^*(z) a_0^{*-1/2}(P)$  and  $V(z, P) = V^*(z) R_y^*(P)$ , respectively.

Within this context, the Schrödinger equation can be written as:

$$-\frac{d^2 \psi^*}{dz^{*2}} + V^* \psi^* = E^* \psi^*. \quad (2)$$

The inclusion of pressure effects is made via the variation of the main input parameters upon  $P$  [18, 37, 38]. At the GaAs  $\Gamma$ -point conduction band minimum, the following relation for the energy band gap holds;

$$E_{\text{gap}}(P) = E_1 + \beta P, \quad (3)$$

where  $E_1 = 1519$  meV, and  $\beta = 10.7$  meV/kbar. The variation of the static dielectric constant is given by [39]:

$$\epsilon(P) = 12.65 e^{-1.67P \times 10^{-3}}, \quad (4)$$

and the corresponding electron effective mass is given by [40–42]:

$$\frac{m_0}{m^*(P, T)} = 1 + E_P^\Gamma \left[ \frac{2}{E_g^\Gamma(P, T)} + \frac{1}{E_{\text{gap}}^\Gamma(P, T) + \Delta_0} \right]. \quad (5)$$

Here  $m_0$  is the free electron mass,  $E_P^\Gamma = 7.51$  eV is the energy related to the momentum matrix element,  $\Delta_0 = 0.341$  eV is the spin-orbit splitting, and  $E_{\text{gap}}^\Gamma(P, T)$  is the pressure and temperature-dependent energy gap for the GaAs quantum well at the  $\Gamma$ -point [41]. The expression for  $E_{\text{gap}}^\Gamma(P, T)$  is

$$E_{\text{gap}}^\Gamma(P, T) = E_{\text{gap}}^\Gamma(0, T) + bP + cP^2, \quad (6)$$

where  $E_{\text{gap}}^\Gamma(0, T) = 1.519 - (5.405 \times 10^{-4} T^2)/(T + 204)$ ,  $b = 0.0126$  eV/kbar, and  $c = 3.7710^{-5}$  eV/kbar<sup>2</sup> [41].

In this work, the variation of  $P$  lies within the range between 0 and 10 kbar. We restrict ourselves to consider values of  $P$  below the point of transition from the direct to the indirect energy gap regimes, induced by pressure in GaAs. In addition, we limit our calculation in this work to temperature  $T=0$  K.

Moreover, the confinement potential can be related to the well known Thomas-Fermi potential through the following relations,

$$V^* = \frac{V(z, P=0)}{R_y^*(P=0)}, \quad (7)$$

where  $V(z, P=0)$  is the  $\delta$ -doped well potential at  $P=0$ , and is described within the self-consistent Thomas-Fermi approach [43] by:

$$V(z, P=0) = -\frac{\alpha_n^2}{(\alpha_n |z| + z_{0n})^4}, \quad (8)$$

with  $\alpha_n = 2/(15\pi)$  and  $z_{0n} = (\alpha_n^3/\pi N_{2d})^{1/5}$ ,  $N_{2d}$  is the two-dimensional impurities density of the  $n$ -type DDQW.

It is worth mentioning that the solution of Eq. (2) gives energy levels  $E_0^*$ , and their corresponding wavefunctions  $\psi_0^*$ . Their correspondence for a value of  $P$  is:

$$E_0(P) = E_0^* R_y^*(P), \quad (9)$$

and

$$\psi_0(P) = \psi_0^* a_0^{*-1/2}(P). \quad (10)$$

After obtaining the subband energies and their corresponding wave functions, the linear refractive index changes ( $\Delta n^{(1)}(\omega)/n_r$ ) and the nonlinear refractive index changes

$(\Delta n^{(3)}(\omega, I)/n_r)$  for the intersubband transitions can be readily calculated as [44, 45]:

$$\frac{\Delta n^{(1)}(\omega)}{n_r} = \frac{|M_{10}|^2 m^* k_B T}{2n_r^2 \epsilon_0 \pi \hbar^2 L_{\text{eff}}} \left[ \frac{(E_f - E_i - \hbar\omega)}{(E_{10}^{\hbar\omega})^2 + (\hbar/\tau_{in})^2} \right] \times \ln \left\{ \frac{1 + \exp[(E_F - E_0)/k_B T]}{1 + \exp[(E_F - E_1)/k_B T]} \right\}, \quad (11)$$

where  $E_{10}^{\hbar\omega} = E_{10} - \hbar\omega$ , and  $E_{10} = E_1 - E_0$  is the main intersubband transition. The third order correction is given by,

$$\frac{\Delta n^{(3)}(\omega, I)}{n_r} = -\frac{\mu c |M_{10}|^2 I}{4n_r^3 \epsilon_0 [(E_{10}^{\hbar\omega})^2 + (\hbar/\tau_{in})^2]^2} \times \frac{m^* k_B T}{\pi \hbar^2 L_{\text{eff}}} \ln \left\{ \frac{1 + \exp[(E_F - E_0)/k_B T]}{1 + \exp[(E_F - E_1)/k_B T]} \right\} \times \left[ 4E_{10}^{\hbar\omega} |M_{10}|^2 - \frac{|M_{11} - M_{00}|^2}{(E_{10})^2 + (\frac{\hbar}{\tau_{in}})^2} \{ \dots \} \right], \quad (12)$$

the term in brackets  $\{ \dots \}$  is given by:

$$\left\{ E_{10}^{\hbar\omega} \left[ E_{10}(E_{10}^{\hbar\omega}) - \left( \frac{\hbar}{\tau_{in}} \right)^2 \right] - \left( \frac{\hbar}{\tau_{in}} \right)^2 [2E_{10} - \hbar\omega] \right\},$$

here,  $E_{10}$  denote the quantized energy level difference for the first excited state and ground state,  $I$  is the optical intensity of incident wave,  $\mu$  is the permeability,  $c$  is the speed of light in free space,  $L_{\text{eff}}$  is the effective spatial extent of electrons in subbands,  $n_r$  is the refractive index and  $\tau_{in}$  is the intersubband relaxation time ( $\tau_{in}$  is a constant, with numerical value 0.14 ps [45, 46]).

The matrix element given by

$$M_{10} = \int_{-L_0/2}^{L_0/2} \psi_1^*(z) z \psi_0(z) dz. \quad (13)$$

Since hydrostatic pressure does not break the symmetry of a symmetric potential configuration [1], then  $M_{11} = M_{00} = 0$ . Therefore, the expression Eq. 12 can be reduced to:

$$\frac{\Delta n^{(3)}(\omega, I)}{n_r} = -\frac{\mu c |M_{10}|^2 I}{4n_r^3 \epsilon_0 \{(E_{10}^{\hbar\omega})^2 + (\hbar/\tau_{in})^2\}^2} \times \frac{m^* k_B T}{\pi \hbar^2 L_{\text{eff}}} \ln \left\{ \frac{1 + \exp[(E_F - E_0)/k_B T]}{1 + \exp[(E_F - E_1)/k_B T]} \right\} \times [4(E_{10}^{\hbar\omega}) |M_{10}|^2], \quad (14)$$

The relative linear refractive index changes  $(\Delta n^{(1)}(\omega, P)/n_r)_{\text{rel}}$  and relative nonlinear refractive index changes  $(\Delta n^{(3)}(\omega, I, P)/n_r)_{\text{rel}}$  are given by:

$$\left( \frac{\Delta n^{(1)}(\omega, P)}{n_r} \right)_{\text{rel}} = \frac{\left( \frac{\Delta n^{(1)}(\omega, P)}{n_r} \right)}{\left( \frac{\Delta n^{(1)}(\Omega, P=0)}{n_r} \right)_{10}}, \quad (15)$$

and

$$\left( \frac{\Delta n^{(3)}(\omega, I, P)}{n_r} \right)_{\text{rel}} = \frac{\left( \frac{\Delta n^{(3)}(\omega, I, P)}{n_r} \right)}{\left( \frac{\Delta n^{(3)}(\Omega, P=0)}{n_r} \right)_{10}}, \quad (16)$$

where  $(\Delta n^{(1)}(\Omega, P=0)/n_r)_{10}$  is the linear refractive index changes for the intersubband transitions between the ground state and the first excited state at  $P=0$  kbar, and  $\Omega = \arg [\max (\Delta n^{(1)}(\omega, P=0)/n_r)_{10}]$  presents the value of resonance for intersubband transition 1-0.

Writing expressions (15) and (16) in relative effective atomic units at  $T=0$  K,

$$\left( \frac{\Delta n^{(1)}(\omega, P)}{n_r} \right)_{\text{rel}} = \frac{m^*(P)\epsilon(0)}{m^*(0)\epsilon(P)} \frac{\Delta E_{10}(P) - \hbar\omega}{\Delta E_{10}(0) - \hbar\omega} \times \left[ \frac{(\Delta E_{10}(0) - \hbar\omega)^2 + (\hbar/\tau_{in})^2}{(\Delta E_{10}(P) - \hbar\omega)^2 + (\hbar/\tau_{in})^2} \right], \quad (17)$$

and

$$\left( \frac{\Delta n^{(3)}(\omega, I, P)}{n_r} \right)_{\text{rel}} = -\frac{2n_r I}{\epsilon_0 c} \left( \frac{\Delta n^{(1)}(\omega, P)}{n_r} \right)_{\text{rel}} \times \frac{1}{(\Delta E_{10}(P) - \hbar\omega)^2 + (\hbar/\tau_{in})^2} \times \left[ |M_{10}(0)|^2 \frac{\epsilon(P) m^{*2}(0)}{\epsilon^2(0) m^{*2}(P)} \right], \quad (18)$$

where  $\Delta E_{10}(P) = \Delta E_{10}(0) \frac{m^*(P)}{m^*(0)} \times \frac{\epsilon^2(0)}{\epsilon^2(P)}$ , furthermore  $\Delta E_{10}(0) = E_1(0) - E_0(0)$  denote the difference between the final state and initial state for  $P=0$  kbar. Now, we define the relative matrix element as:

$$M_{10\text{rel}} = \frac{M_{10}(P)}{M_{10}(0)}, \quad (19)$$

which can be written in effective atomic units as,

$$M_{10\text{rel}} = \frac{m^*(0)}{m^*(P)} \times \frac{\epsilon(P)}{\epsilon(0)}. \quad (20)$$

Finally, using Eqs. (11), (12), (17) and (18), one can express the relative total refractive index change  $(\Delta n^{(\text{tot})}(\omega, I, P)/n_r)_{\text{rel}}$  as:

$$\left( \frac{\Delta n^{(\text{tot})}(\omega, I, P)}{n_r} \right)_{\text{rel}} = \left( \frac{\Delta n^{(1)}(\omega, P)}{n_r} \right)_{\text{rel}} + \left( \frac{\Delta n^{(3)}(\omega, I, P)}{n_r} \right)_{\text{rel}}. \quad (21)$$

Therefore, the effect of hydrostatic pressure on these optical properties (Eqs. (17) and (18)) can be written in terms of the mass and the dielectric constant, which are pressure dependent.

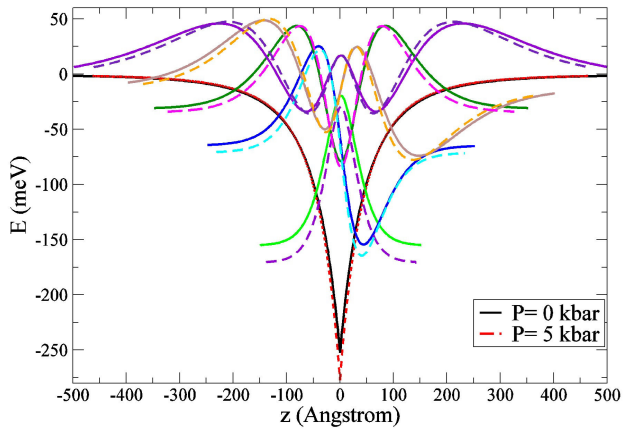


FIGURE 1. Confining  $\delta$ -potential profile and subband energies with their wave functions for  $P = 0$  kbar (Solid curves) and  $P = 5$  kbar (Dashed curves) for  $N_{2d} = 7.5 \times 10^{12} \text{ cm}^{-2}$ .

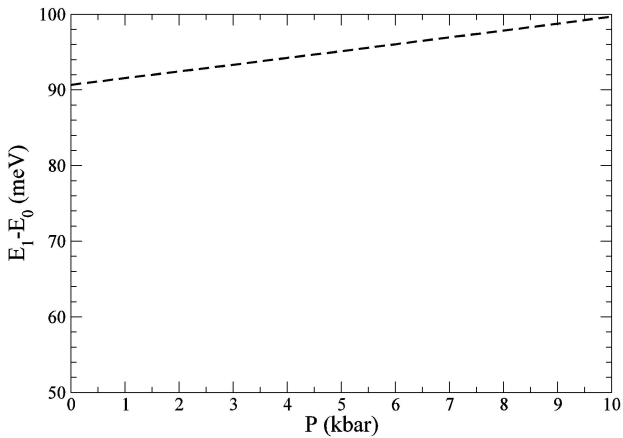


FIGURE 2. Energy difference between ground state and first excited state as a function of hydrostatic pressure for  $N_{2d} = 7.5 \times 10^{12} \text{ cm}^{-2}$ .

### 3. Results and Discussion

We have theoretically investigated the linear and nonlinear refractive index changes for the intersubband transition (1-0) in DDQW. Figure 1 displays the confinement potential profile, subband energy levels and wave functions associated to these energy levels in DDQW, for a doping concentration  $N_{2d} = 7.5 \times 10^{12} \text{ cm}^{-2}$ . Solid (dashed) curves correspond to  $P = 0$  ( $P = 5$  kbar). By increasing the pressure the potential is more attractive and the associated wave function more compressed and localized. This behavior was also observed in quantum dots under hydrostatic pressure [33]. To this respect, it is well known that application of hydrostatic pressure turns out in a modification of the physical properties [40,47,48], mainly due to deformation of the interatomic bonds [49]. As pressure increases, the dielectric constant decreases and the effective mass increases [40] leading to a decreasing in effective Bohr radius and an increasing in the effective Rydberg [1]. So, electrons are more confined and localized, see Eq. (9) and Eq. (10).

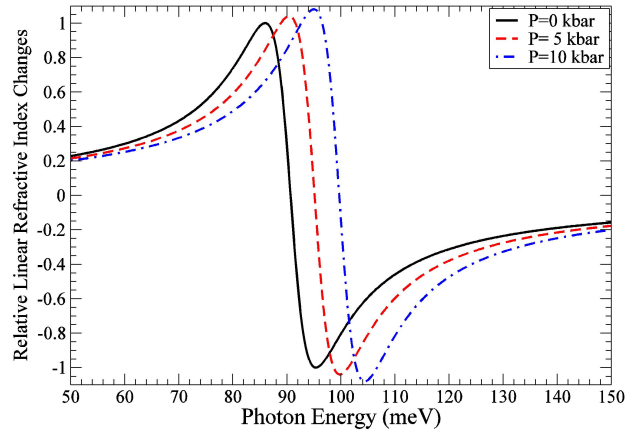


FIGURE 3. Relative linear refractive index changes as a function of the photon energy for (1-0) intersubband transition for (a)  $P=0$  kbar, (b)  $P=5$  kbar and (c)  $P=10$  kbar. The bidimensional density is  $N_{2d} = 7.5 \times 10^{12} \text{ cm}^{-2}$ .

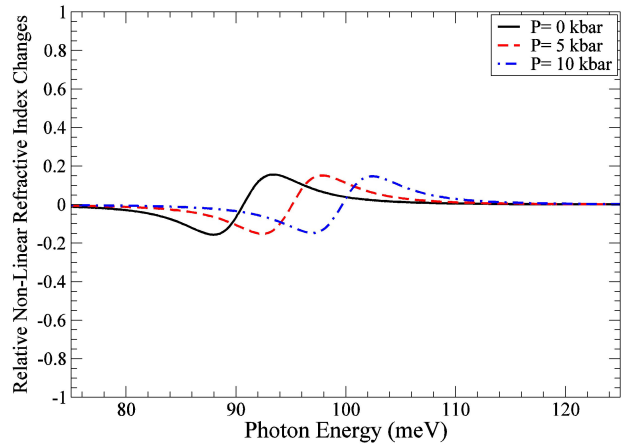


FIGURE 4. Relative nonlinear refractive index changes of the (1-0) intersubband transition as a function of the photon energy for  $P = 0, 5, 10$  kbar with  $I = 0.5 \text{ MW/cm}^2$  and  $N_{2d} = 7.5 \times 10^{12} \text{ cm}^{-2}$ .

Figure 2 shows the energy difference between the first excited state and the ground state as a function of pressure. Here, it can be observed that the energy difference increases when the pressure increases as well. A similar behavior was observed in V-groove quantum wires [4].

In Fig. 3, the linear refractive index changes are plotted as a function of photon energy for three different pressures, 0, 5 and 10 kbar, with  $I = 0.5 \text{ MW/cm}^2$ . When the pressure increases, the linear RIC shifts toward higher energies. The main reason for this shift is the increment in energy difference between the ground state and first excited state, by increasing the pressure (Fig. 2). Taking into account Eq. 11, we can see that the function in the second factor on the right-hand side has two structures centered at  $\hbar\omega = \pm\Delta E = \pm(E_1 - E_0)$ . Therefore, in Fig. 3 there are two resonant peaks in each curve. Also, it is observed that the peak of the linear RIC increases as pressure increases. This behavior results from a modification of the physical properties as the pressure increases. Mainly, when the pressure increases, the dielectric

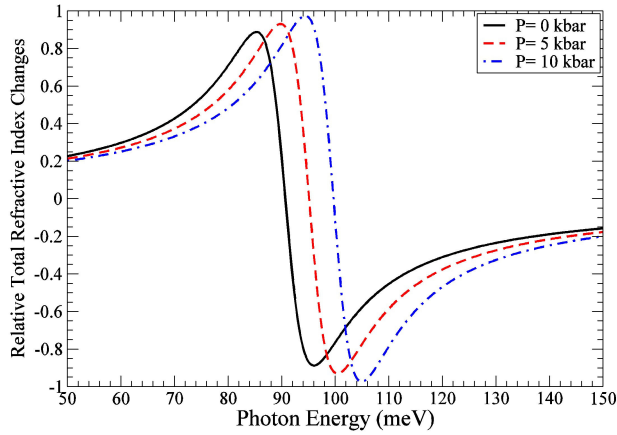


FIGURE 5. Variation of the total relative refractive index changes as a function of the photon energy for three different pressures (a)  $P = 0$  kbar, (b)  $P = 5$  kbar and (c)  $P = 10$  kbar with for  $I = 0.5$  MW/cm<sup>2</sup>.

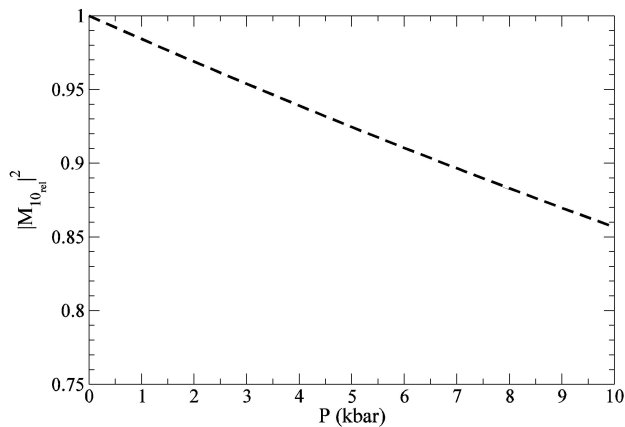


FIGURE 6. Square dipole matrix element for intersubband transitions between the ground state and the first excited state versus hydrostatic pressure for  $N_{2d} = 7.5 \times 10^{12}$  cm<sup>-2</sup>.

constant decreases and the effective mass increases [40] leading to an increasing in the relative linear RIC (see Eq. (17)).

Figure 4 displays the nonlinear RIC as a function of photon energy for three different pressures with  $I = 0.5$  MW/cm<sup>2</sup>. It is seen that the nonlinear RIC shifts toward higher energies as pressure increases, in agreement with Fig. 2.

In Fig. 5, the total RIC as a function of the incident photon energy for three different hydrostatic pressure values with  $I = 0.5$  MW/cm<sup>2</sup> is shown. As can be seen in this figure, for a constant incident optical intensity, as the hydrostatic pressure increases the magnitude of the total RIC increases and also shifts toward higher energies. The shift is compatible with other quantum structures [4, 31]. Those results have similar behavior with linear refractive index changes. The main reason for this behavior comes from changes in quantum confinement as hydrostatic pressure increases. The quantum confinement change causes an increment of the electron energy difference between the lowest two subbands, where an optical transitions occurs.

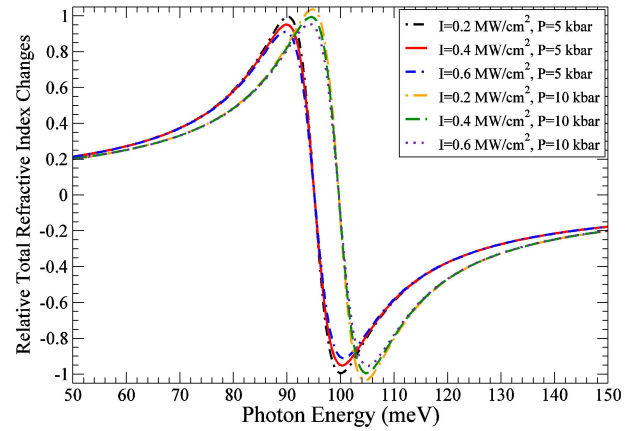


FIGURE 7. Total relative refractive index changes versus the photon energy for different optical intensities  $I = 0.2, 0.4, 0.6$  MW/cm<sup>2</sup> under hydrostatic pressure  $P = 5, 10$  kbar.

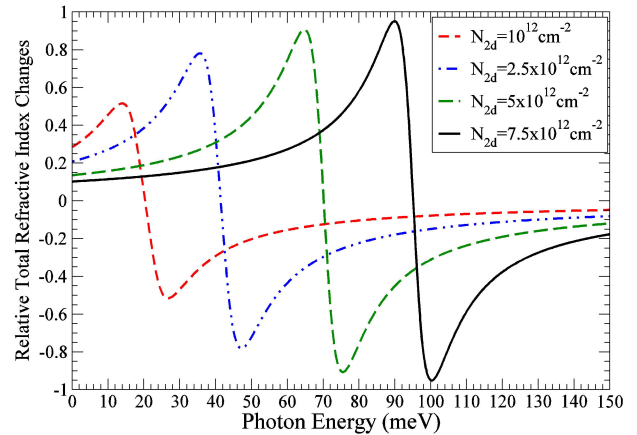


FIGURE 8. Total relative refractive index changes as a function of the photon energy for different values of bidimensional density  $N_{2d} = 1, 2.5, 5, 7.5 \times 10^{12}$  cm<sup>-2</sup> with an optical intensity  $I = 0.5$  MW/cm<sup>2</sup> and under hydrostatic pressure  $P = 5$  kbar.

We show the square dipole matrix elements as a function of pressure in Fig. 6. As we can see, the dipole matrix elements decrease with increasing pressure. This kind of result was also found in quantum dots [33] and simple quantum wells [32] under hydrostatic pressure.

In Fig. 7 the total RIC is plotted as functions of the photon energy for different incident optical beam intensities as well as for two values of hydrostatic pressure. RIC peaks show a blue-shift and a significant enhancement as hydrostatic pressure increases. On the other hand, total RIC decreases as the incident optical beam intensity increases. This drop was also observed in simple quantum wells under pressure [50]. Moreover, the higher optical intensity will, indeed, cause a decrease in the nonlinear term, while the linear term does not change with beam intensity (see Eq. 11 and Eq. 17). Because these two terms are opposite in sign, any increase the incident optical intensity will increase the magnitude of the nonlinear term, on the contrary reducing the net  $(\Delta n^{(\text{tot})}(\omega, I, P)/n_r)_{\text{rel}}$ .

Keeping the beam intensity at a constant value  $I = 0.5 \text{ MW/cm}^2$  and  $P = 5 \text{ kbar}$ , we have investigated the effect of doping density on the total RIC, see Fig. 8. The total RIC is plotted as a function of photon energy for different values of bidimensional density. The total refractive index increases and also shifts toward higher energies as the doping concentration increases. Similar results have been reported in AlGaIn/GaN quantum well heterostructures [2,5] and in delta-doped quantum well [50].

If we compare Fig. 8 and Fig. 5 we can see that the changes in concentration have a much stronger effect on refractive index than the changes of pressure. Therefore, if it is desired to achieve a large change in the refractive index, high bidimensional densities are recommended.

As a final remark, it is important to discuss, some aspects that can be relevant from the experimental standpoint. It is well known that the peaks in the absorption spectra can be readily distinguished by their polarization sensitivity [51,52]. In particular, the peaks associated to the intersubband processes, can be distinguished using light with polarization perpendicular to the quantum well plane. On the contrary, the peaks related to intrasubband processes can be favoured when the light is polarized parallel to the quantum well plane. It is also known that the optical properties are pretty sensitive to temperature, so different mechanisms such as plasma oscillations and hot-electron bolometric effect have been proposed to explain the absorption peaks associated to intrasubband processes [52, 53]. Specifically, at room temperature the plasma oscillation model explains quite well peaks sensitive to light polarized parallel to the quantum well plane,

intrasubband processes [52]. In our case, these details about intrasubband processes are even more important due to the indirect character (quantum well for electrons and barrier for holes) of the delta-doped quantum wells. Within this context, further studies of the polarization sensitivity and temperature dependence of the optical properties in delta-doped quantum wells are needed. Even more, experimental works are required in order to unveil: firstly the linear and nonlinear optical properties, secondly if the subband processes involved are of intrasubband or intersubband character, and thirdly if the plasma oscillation model or the hot-electron bolometric effect can explain the experimental outputs.

#### 4. Conclusions

In the present work, we obtained a new algebraic expression of the linear and nonlinear RIC, under hydrostatic pressure in DDQW. The linear and nonlinear RIC under hydrostatic pressure can be explained through the pressure dependence of the effective atomic units. Our results obtained with theoretical model of pressure show that the linear RIC is not related to the incident optical intensity, whereas the incident optical intensity has a great influence on the nonlinear change. Moreover, the total RIC will be reduced as the incident optical intensity increases. Additionally, we have shown that increasing the hydrostatic pressure, the refractive index spectrum is blue-shifted and changed in magnitude. Our model is very simple to implement and it can reproduce results of other approaches. Our calculations also reveal that RIC is very sensitive to the bidimensional density of DDQW.

- 
1. O. Oubram, O. Navarro, L. M. Gaggero-Sager, J. C. Martínez-Orozco and I. Rodríguez-Vargas, *Solid State Sci.* **14** (2012) 440.
  2. I. Saidi, L. Bouzaïene, H. Maaref and H. Mejri, *J. Appl. Phys.* **101** (2007) 094506.
  3. F. Urgan, U. Yesilgul, E. Kasapoglu, H. Sari and I. Sökmen, *J. Lumin.* **132** (2012) 1627.
  4. R. Khordad, S. Kheiryazadeh Khaneghah and M. Masoumi, *Superlattice Microst.* **47** (2010) 538.
  5. I. Saidi, L. Bouzaïene, H. Mejri and H. Maaref, *Mat. Sci. Eng. C* **28** (2008) 831.
  6. L. C. West and S. J. Eglash, *Appl. Phys. Lett.* **46** (1985) 1156.
  7. R. J. Turton and M. Jaros, *Appl. Phys. Lett.* **54** (1989) 1986.
  8. D. Ahn and S. L. Chuang, *Phys. Rev. B* **35** (1987) 4149.
  9. D. Ahn and S. L. Chuang, *Phys. Rev. B* **34** (1986) 9034.
  10. G. Sun and J. B. Khurgin, *IEEE J. Quantum Electron.* **29** (1993) 1104.
  11. E. Ozturk, Y. Ergun, H. Sari, I. Sokmen, *Semicond. Sci. Technol.* **16** (2001) 421.
  12. M. E. Mora-Ramos, L. M. Gaggero-Sager and C. A. Duque, *Physica E* **44** (2012) 1335.
  13. S. Liang and W. Xie, *Physica B* **406** (2011) 2224.
  14. G. Liu, K. Guo and Ch. Wang, *Physica B* **407** (2012) 2334.
  15. L. M. Gaggero-Sager, G. G. Naumis, M.A. Muñoz-Hernandez and V. Montiel-Palma, *Physica B* **405** (2010) 4267.
  16. V. Grimalsky, L.M. Gaggero-Sager and S. Koshevaya, *Physica B* **406** (2011) 2218.
  17. S. J. Vlaev, I. Rodriguez-Vargas and L. M. Gaggero-Sager, *Phys. Status Solidi C* **2** (2005) 3649.
  18. O. Oubram, M. E. Mora-Ramos and L. M. Gaggero-Sager, *Eur. Phys. J. B* **71** (2009) 233.
  19. E. Ozturk, M. K. Bahar, I. Sokmen, *Eur. Phys. J. Appl. Phys.* **41** (2008) 195.
  20. J. C. Martínez-Orozco, M. E. Mora-Ramos and C. A. Duque, *Phys. Status Solidi B* **249** (2012) 146.
  21. J. C. Martínez-Orozco, M. E. Mora-Ramos and C. A. Duque, *J. Lumin.* **132** (2012) 449.
  22. İ. Karabulut, M. E. Mora-Ramos and C. A. Duque, *J. Lumin.* **131** (2011) 1502.
  23. J.G. Rojas-Briseño, J.C. Martínez-Orozco, I. Rodríguez-Vargas, M.E. Mora-Ramos, C.A. Duque, *Physica B* **424** (2013) 13.

24. E. Ozturk, I. Sokmen, *J. Lumin.* **134** (2013) 42.
25. B. Piechal, J. W. Tomm, A. Bercha, W. Trzeciakowski, M. Reufer and A. Gomez-Iglesias, *Appl. Phys. A* **97** (2009) 179.
26. F. Dybala, A. Bercha, P. Adamiec, R. Bohdan and W. Trzeciakowski, *Phys. Status Solidi B* **244** (2007) 219.
27. W. Trzeciakowski, A. Bercha, F. Dybaa, R. Bohdan, P. Adamiec and O. Mariani, *Phys. Status Solidi B* **244** (2007) 179.
28. M. Maziarz, B. Piechal, A. Bercha, R. Bohdan, W. Trzeciakowski and J. A. Majewski, *Acta Phys. Pol. A* **112** (2007) 437.
29. M. Bajda, B. Piechal, F. Dyba, A. Bercha, W. Trzeciakowski and J. A. Majewski, *Phys. Status Solidi B* **249** (2012) 217.
30. H. M. Baghranyan, M. G. Barseghyan, C. A. Duque and A. A. Kirakosyan, *J. Phys. Conf. Ser.* **350** (2012) 012016.
31. M. Santhi, A. John Peter and C. K. Yoo, *Superlattice Microst.* **52** (2012) 234.
32. N. Eseanu, *Phys. Lett. A* **374** (2010) 1278.
33. R. Khordad, G. Rezaei, B. Vaseghi, F. Taghizadeh and H. Azadi Kenary, *Opt. Quant. Electron.* **42** (2011) 587.
34. E. Ozturk, I. Sokmen, *J. Lumin.* **134** (2013) 42.
35. A. Hakimyard, M. G. Barseghyan and A. A. Kirakosyan, *Physica E* **41** (2009) 1596.
36. M. Nazari, M.J. Karimi, A. Keshavarz, *Physica B* **428** (2013) 30.
37. N. Raigoza, A. L. Morales, A. Montes, N. Porrás-Montenegro and C. A. Duque, *Phys. Rev. B* **69** (2004) 045323.
38. W. Trzeciakowski and M. Baj, *Solid State Commun.* **5** (1984) 669.
39. M. G. Barseghyan, A. Hakimyard, S. Y. López, C. A. Duque and A. A. Kirakosyan, *Physica E* **43** (2010) 529.
40. E. Kasapoglu, F. Ungan, H. Sari and I. Sökmen, *Physica E* **42** (2010) 1623.
41. H. Ehrenrich *J. Appl. Phys.* **32** (1961) 2155.
42. D. E. Aspnes, *Phys. Rev. B* **14** (1976) 5331.
43. L. Ioriatti, *Phys. Rev. B* **41** (1990) 8340.
44. S. Ünü, İ. Karabulut and H. Şafak, *Physica E* **33** (2006) 319.
45. D. Ahn and S. L. Chuang, *IEEE J. Quantum Elect.* **23** (1987) 2196.
46. E. Ozturk and I. Sokmen, *Solid State Commun.* **126** (2003) 605.
47. P. Nithiananthi and K. Jayakumar, *Phys. Status Solidi B* **246** (2009) 1238.
48. X. L. Wang, M. Y. Nia, Z. Zeng and H. Q. Lin, *J. Magn. Magn. Mater.* **321** (2009) 2575.
49. P. Yu and M. Cardona, *Fundamentals of Semiconductors* (Springer, Berlin, 2005).
50. E. Ozturk, Y. Ozdemir, *Opt. Commun.* **294** (2013) 361.
51. L. H. Peng and C. G. Fonstad, *Appl. Phys. Lett.* **63** (1993) 1534.
52. J. M. Li, K. Y. Qian, Q. S. Zhu and Z. G. Wang, *Appl. Phys. Lett.* **90** (2007) 162111.
53. E. Rosencher, E. Martinet, E. Bockenhoff, Ph. Bois, S. Delaitre and J. P. Hirtz, *Appl. Phys. Lett.* **58** (1991) 2589.